International Journal of Enhanced Research in Science Technology & Engineering, ISSN: 2319-7463
Vol. 3 Issue 2, February-2014, pp: (214-220), Impact Factor: 1.252, Available online at: www.erpublications.com

Systematic investigation of the effect of oxidation on the structure of Single-Walled Carbon Nanotubes (SWNTs)

Shahir Hussain, Sakshi Sharma
Department. of Applied Sciences and humanities,
Faculty of Engineering and Tech., Jamia Millia Islamia, India

---

Abstract: Purification of single-walled carbon nanotubes (SWNTs) is still remaining a challenging task. The aim of this work is to show novel and fast concepts for the purification of CNTs by combination of different techniques and analyses the effect of that methods on the carbon nanotubes. The carbonaceous particles were presumably etched away by the selective oxidation with faster etching rate than nanotubes. This gives rise to very high yield of about 35%. The oxidation procedure was characterized by using Raman spectroscopy, infrared spectroscopy and scanning electron microscopy (SEM). It was found from Raman scattering measurements that the ratio of the intensity of G-line peak to that of D-line peak increased drastically by this purification process. The D–G ratio of dynamically air oxidized SWNTs (0.06) is much smaller than that of as-received (0.09) or air–HCl purified (0.1) SWNTs, indicating higher purity (and lower level of structural defects) of the dynamically air oxidized sample. The results reveal that the different functional groups can be introduced when the SWNTs are treated with different oxidants. Refluxing in dilute nitric acid introduce the carboxylic acid groups only at those initial defects that already exist. It is confirm by Fourier Transform Infrared spectroscopy (FTIR).

---

1. Introduction

With the discovery of Carbon nanotubes (CNTs) in 1991, have attracted attention of scientist worldwide, [1] due to their unique structure and potential properties. These unique properties make them the most promising candidate for the building blocks of molecularscale machines and nanoelectronic devices. The electronic structure of CNT can be either metallic or semiconducting, depending on their diameter and chirality [2]. These diverse electronic properties open a possibility of developing nanoelectronic devices as nanowires [3]. But a large amount of unwanted carbon particles such as amorphous, graphitic nanoparticle and some catalysis are present in the soot in addition to carbon nanotubes. These impurities effect the properties of nanotubes and performance of the devices fabricated. High level purified nanotubes are required for sophisticated measurement and practical.

In this paper we study the chemical effect on SWNTs surface during purification by annealing and acid treatment. The morphology of SWNTs and degree of purification were observed by scanning electron microscope (SEM). Fourier transform Infrared (FTIR) spectroscopy evident the attachment of functional group on the surface on carbon nanotubes during chemical treatment. Raman spectroscopy was used to confirm the formation of graphitized carbon nanotubes and to investigate qualitatively the degree of purification.

2. Experimental

15 mg of raw SWNTs (pristine tubes) were loaded into a ceramic inner container, and placed into a furnace, and heated at 350 ^{0}C for 1hr to oxidize Fe nanoparticles. An oxidative treatment of raw SWNTS material is effective in removing non-nanotube carbon and exposing the metal catalysts by removing carbon coating. However, nanotubes can be lost or damaged during the oxidation process. It is desirable that a scalable cleaning method only removes carbon impurities and metal catalysts without damaging nanotubes The annealed tubes were immersed into 120 mL concentrated (6 M) HCl and (6 M) HNO_3 (70%) solution. Then the sample was refluxed for 6 h with stirring. After cooling down the sample, it was diluted and washed several times with DI water and then filtered onto a 0.22 m pore size cellulose membrane under vacuum and washed several times with DI water until pH 6-7 was reached. Tubes were collected and dried in an oven at 60 ^{0}C overnight. After rinsing and drying the sample, a grayish black, thin mat composed of SWNTs was finally obtained.

3. Characterizations

All samples were characterized by Raman spectroscopy, Fourier Transform Infrared spectroscopy (FTIR) and Scanning Electron Microscopy (SEM).

3.1 The purity estimation of SWNTs by Raman spectroscopy

Raman spectroscopy was employed to identify changes of the raw and purified samples. Raman spectra of as-received, air oxidized, air–HCl purified and air–HNO_3 purified SWNTs are presented in fig.1. All samples show the typical Raman features of SWNTs: the disorder-induced band (1300–1400 cm^{-1}) resulting from amorphous carbon and structural defects in SWNTs; the G band (~1590 cm^{-1}) originating from the in-plane vibrations of carbon–carbon bonds; and Carbon nanotubes also exhibit a unique, low frequency, first-order Raman scattering feature identified with the radial breathing mode of the tube wall.

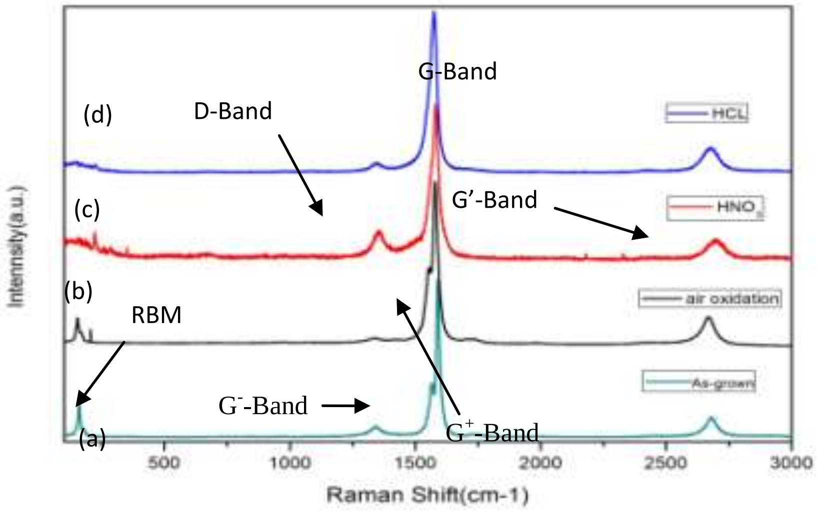

Figure 1: Raman spectra of (a) as-grown, (b) air oxidized, (c) air-HCL purified and (d) air-HNO_3 purified SWNTs

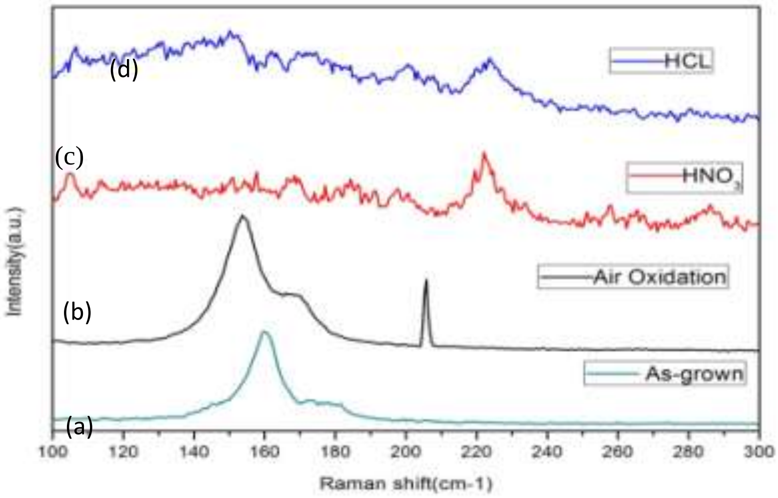

Figure 2: RBM band Raman spectra of (a) as-grown, (b) air oxidized, (c) air-HCL purified and (d) air-HNO3 purified SWNTs

However, after the acid treatment (second step of the purification process), the relative integrated intensity of the D-band increases, and the D-band broadens (fig.1(c) and (d) and fig. 3(c) and (d)). The increase in the D-band intensity and broadening after acid treatment is the verification of an increase in structural disorder in the SWNTs bundles. Using the D-band as a probe, it is clear from comparing the spectra in (fig. 3(d) - HCl reflux) and (fig.3 (c) - HNO_3 reflux), that HNO_3 induces significantly more chemical change to the air oxidized nanotubes. However, the broadening is obviously quite strong, and the substructure within the G-band (G^-) almost disappears which was present in the as-grown and air oxidized samples [7]27**]**.

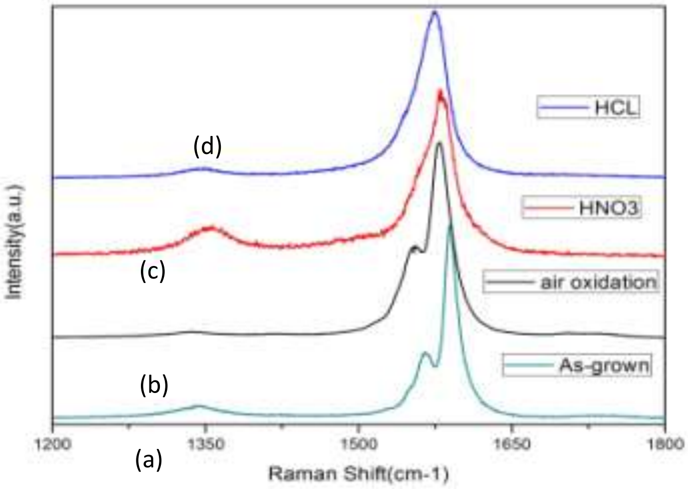

Figure 3: D-G band Raman spectra of (a) as-grown, (b) air oxidized (c) air-HCL purified and (d) air-HNO_3 purified SWNTs

The Raman spectrum of dynamically air oxidized SWNTs revealed a low D band and a high G band intensity with well separated G^- and G+ sub-bands (fig.1(a)&(b)). Table 1 shows, the D–G ratio of dynamically air oxidized SWNTs (0.06) is much smaller than that of as-received (0.09) or air–HCl purified (0.1) SWNTs, indicating higher purity (and lower level of structural defects) of the dynamically air oxidized sample (fig. 1b). The maximum of the RBM intensity is shifted to lower frequencies, probably because of the oxidation of small-diameter SWNTs which exhibit larger RBM frequencies. In figure 2 (a&b), the intensities of the peaks at 154 cm^{-1} and at 167 cm^{-1} are increase in comparison with the pristine tubes, after air oxidation.

Table 1 shows the different band of Raman spectra with quality factor and intensity ratio of D-to G- band.

Sample	**RBM**	**D-band peak position (cm^{-1})**	**G-band peak position (cm^{-1})**	**G^--band peak position (cm^{-1})**	**G'-band peak position (cm^{-1})**	**I_D/I_G**	**Q-factor**	**Processing**
As-grown	160,173	1344	1588	1567	2681	0.09	0.95	Procured Carbon Nanotechnologyies Inc.(USA)
Air oxidation	154,167, 206	1345	1580	1552	2671	0.06	0.97	Annealing at 350°C in air environment
HNO_3	104,152, 168,183, 222,351	1354	1582	-	2695	0.29	0.88	Annealing + HNO_3 reflux
HCL	106,150, 200,223	1347	1574	-	2677	0.1	0.97	Annealing + HCl reflux

For the HNO_3-based treatment, carboxylic groups have been reported as the most abundant functional group on the carbon nanotubes surface [8,10]. The identification of functional groups attached to the tube walls after HNO_3 reflux will be discussed in next section. Zhang et al. [9] have proposed that the oxidation process begins with the oxidation of initial wall defects (step 1) (e.g., at - CH_2 and –CH groups, or pentagon-heptagon pair defects). These defects might be present, to some extent, after growth, i.e., before or after chemical processing. After these defects are oxidized, they have suggested two more successive steps in the evolution of the defect structure: the defect-generating step (step 2) and the defect consuming step (step 3).

3.1.1 Quality Analysis

The Raman Quality Factor (Q) is a measure of overall quality and particularly indicative of the level of amorphous carbon relative to that of carbon nanotubes given in figure 4. The Raman Quality Factor is defined as:

$$Q = 1 - \frac{(D - B)}{(G - B)}$$

Where:
D = maximum Intensity of D band
G = maximum Intensity of G^+ band
B = baseline, lowest point between the two bands

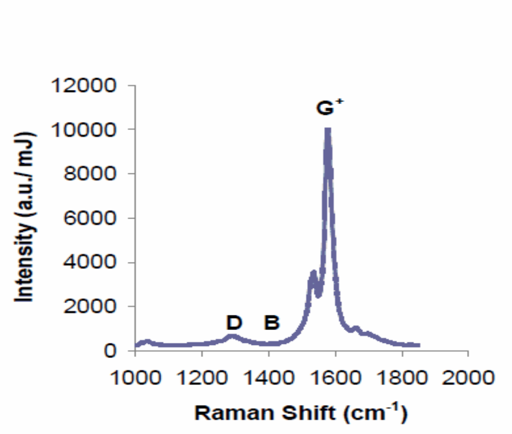

Figure 4: Raman Spectrums for SWNTs

From our samples we seen that quality of the samples is improve as comparison to the as- grown samples as shown in the table 1. Only the gas phase + HNO_3 treated sample (0.88) has lower quality in comparison to pristine sample (0.95), decrease in the quality of HNO_3 treated sample may be due to the destruction of the SWNTs structure during the chemical treatment as we know that Nitric acid is the heavy oxidant in comparison to HCL.

3.2 FTIR of as grown and Modified SWNTs

FTIR is the most powerful tool for identifying types of chemical bonds (functional groups). It can be utilized to quantitative some components of an unknown mixture. We consider first the IR spectrum of the raw soot (Fig. 5 (a)). Many bands from functional groups can be seen in Fig. 5 (b) and (c). For example, the 1382 cm^{-1} band in Fig. 5 (a) is located within the range expected for C-O stretching modes in ethers, esters, alcohols or phenol compounds, and the 1640 cm-1 band can be assigned to carbonyl (C=O) stretching in ketones, aldehydes or carboxylic acid groups [11-13]. However, these high frequency bands are not observed, so the 1710 cm^{-1} band is probably associated with either ketone or carboxylic acid groups. A prominent broad band (3100 - 3600 cm^{-1}) can be observed in many of the IR spectra of fig. 5. This broad band is assigned to contributions from a variety of O-H stretching modes. The width indicates that several different - OH containing groups are probably present in many different chemical and carbon environments. Since the -OH stretch band is present, the C=O band at 1640 cm^{-1} should probably be identified with carboxylic acid groups. Zhang et al. [9] and Kukovecz et al. [14] did not observe a band at ~1700 cm^{-1} in their raw soot samples. For our HCL- processed sample, the IR spectrum (fig. 5(c)) exhibits enhanced absorption near ~ 1710 cm^{-1}. This is consistent with the formation of additional carboxyl groups on the SWNTS surface. The band in the HCL processed material is enhanced to 1710 cm^{-1}, relative to its counterpart in the raw soot (~1640 cm^{-1}) .

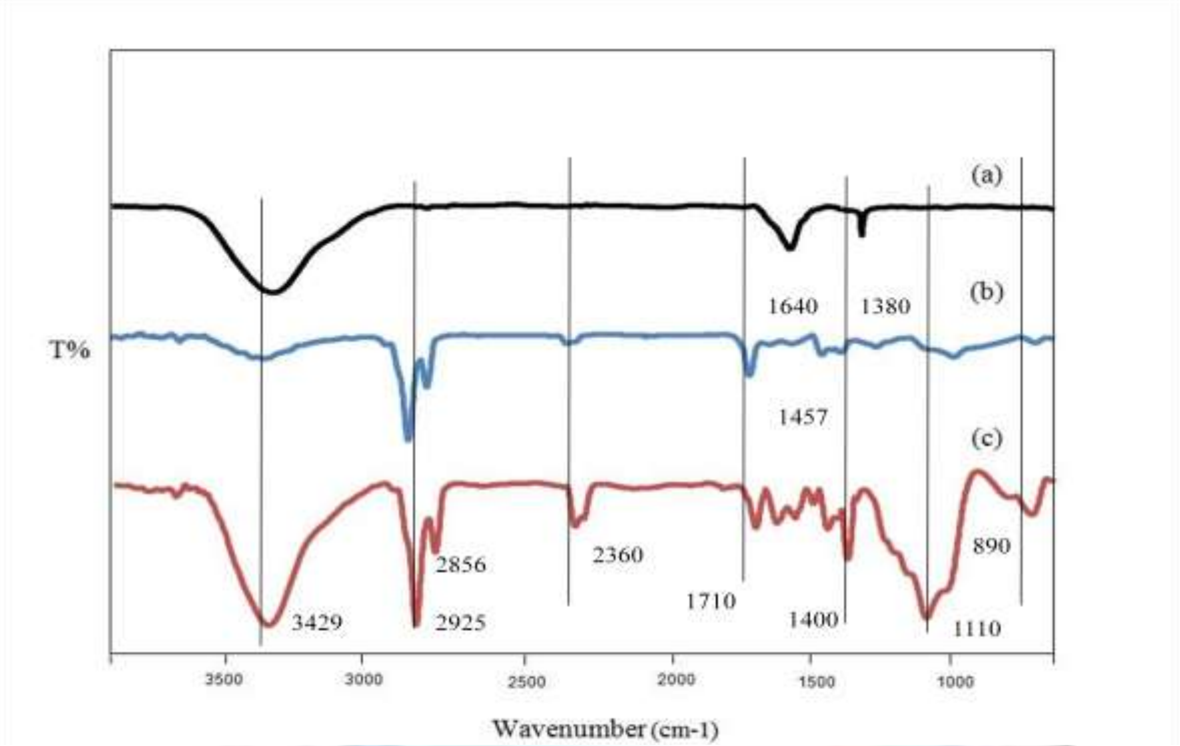

Figure 5: FTIR Spectra of (a) as-grown, (b) HCL and (c) HNO_3 treated SWNTs

After HCL reflux, very broad bands also appear in the ~ 3230 – 3500 cm^{-1} range, and identified with O-H stretching modes. The broad low frequency component of this O-H band with a peak at ~ 3429 cm^{-1} (lower in intensity) is identified with O-H stretching from coupled carboxylic acid groups. The low frequencies observed for both broad -OH bands in fig. 5(b) may be the result of coupling to adjacent O-containing groups. The C-O stretching vibrations in alcohols and phenols also exhibit bands in the 1000- 1260 cm^{-1} range; their frequency depends on the details of the coupling to C-C stretching vibrations. The bands at ~ 1035 cm^{-1} and 1100 cm^{-1}, shown in the spectrum of fig 5(c), could therefore be tentatively identified with C-C-O stretching in unsaturated hydroxyl groups, and the peak appearing at ~ 1400 cm^{-1} in fig. 5 (c) might be associated with the characteristic vibrational mode resulting from interaction between O-H bending and C-O stretching in phenol groups [15].

It seems conclusive from an IR band analysis that an acid reflux approach to AC removal leads to a substantial increase in carboxylic acid and hydroxyl (phenolic and alcoholic) groups relative to the amount found in the raw soot. We analyses the acid processing of SWNTs material to remove the metal growth catalyst.

3.3 Scanning Electron Microscope (SEM)

Morphology Characterization:

Figure 6a shows a SEM image of the as grown SWNTs samples. In addition to the bundle of SWNTs, the white spot, carbonaceous particles, mainly amorphous carbons, are shown in the figure 6(a). Furthermore, we can see that the metal particles were mainly embedded in larger amorphous carbons, as evidenced in Figure 6(a). This sample was thermally annealed at 350 °C for 60 min in air to remove selectively the amorphous carbons. The SEM image of oxidized SWNTs is shown in Figure 6b. The figure shows a dramatic decrease of amorphous carbons after oxidation. As a result of oxidation, the weight of the soot was reduced to about 40 wt % of the original sample.

The basic idea of the selective etching is that amorphous carbons can be etched away more easily than SWNTs due to the faster oxidation reaction.The transition metals can be etched away by an acid treatment. Figure 7(c) and (d) shows the SEM image of the HCL and HNO_3 treated sample, where the annealed sample was immersed in 6M hydrochloric acid (HCL) and 6M Nitric acid(HNO_3) for 6 h respectively .

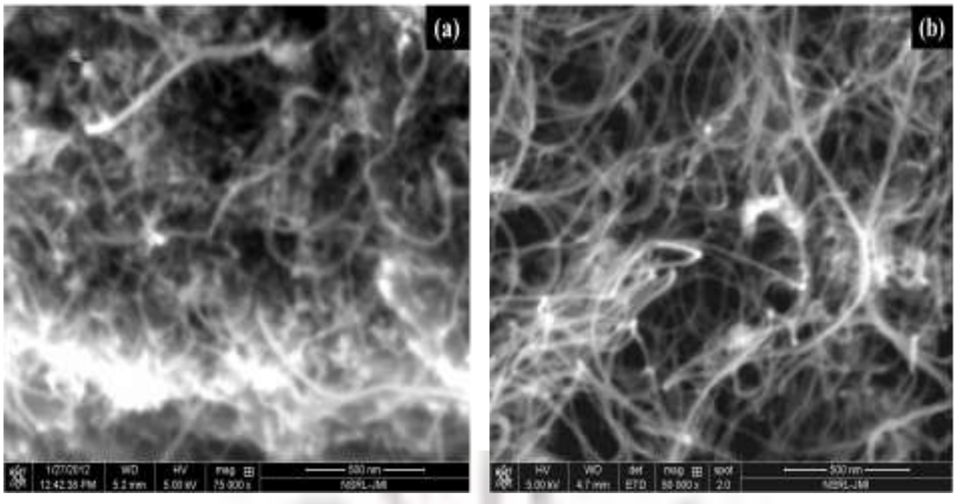

Figure 6 SEM Images of (a) as-grown and (b) air oxidized SWNTs

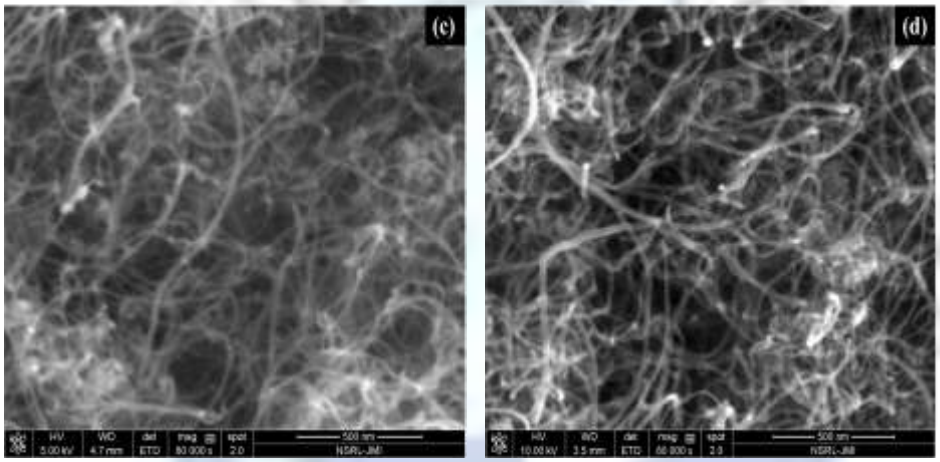

Figure 7 SEM Images of (c) Air oxidation plus HCL and (d) air oxidation plus HNO_3 treated SWNTs

Yet some carbonaceous particles, which are left during the annealing procedure, still remain in the sample, as illustrated in Figure 7(c) and (d). Special care should be taken to obtain better purified samples. We note that the acid treatment enhances the bundling of SWNTs, as shown in Figure 7 (c) and (d), as compared to the annealed samples in Figure 6(a), since the entangled SWNTs are released in acid and aggregated themselves by the van der Waals interactions.

4. Conclusion

The D–G ratio of dynamically air oxidized SWNTs (0.06) is much smaller than that of as-received (0.09) or air–HCl purified (0.1) SWNTs, indicating higher purity (and lower level of structural defects) of the dynamically air oxidized sample. The maximum in the RBM intensity is shifted to lower frequencies, probably because of the oxidation of small-diameter SWNTs which exhibit larger RBM frequencies.

Reference

[1] E. T. Thostenson, Z. F. Ren and T. W. Chou, Composites Science and Technology,Vol. 61, Issue 13, pp. 1899-1912(2001).
[2] S. Niyogi, M.A. Hamon, H. Hu, B. Zhao, P. Bhowmik, R. Sen, M.E.Itkis, and R.C. Haddon, Acc. Chem. Res., Vol.35 (12), pp 1105–1113(2002).
[3] L.A.Girifalco, M. Hodack, and R.S Lee, Phys. Rev. B, vol.62, pp.13104–13110(2000).
[4] S. Osswald, E. Flahaut and Y. Gogotsi, Chem. Mater., 18(6), 1525–1533(2006).
[5] M. S. Dresselhaus, G. Dresselhaus, A. Jorio, A. G. Souza and R. Saito, Carbon, 40(12), 2043–2061(2002).
[6] S. Osswald, E. Flahaut, H. Ye and Y. Gogotsi, Chem. Phys. Lett., 402(4–6), 422–427(2005).

[7] A. M. Rao, E. Richter, S. Bandow, B. Chase, P. C. Eklund, K. A. Williams, S. Fang, K. R. Subbaswamy, M. Menon, A. Thess, R. E. Smalley, G. Dresselhaus and M. S. Dresselhaus, 275(5297), 187–191(1997).
[8] M. Terrones et al., Annu. Rev. Mater. Res., 33, 419–501(2003).
[9] J.Zhang et al., J. Phys. Chem. B, 107: p. 3712(2003).
[10] Kuznetsova A, et al., J. Am. Chem. Soc., 123: p. 10699(2001).
[11] K.Kinoshita, Carbon: Electrochemical and Physicochemical Properties, New York: Wiley &Sons (1988).
[12] P.Fanning and A. V. Ma, Carbon, 31: P. 721(1993).
[13] B.K.Pradhan and N.K. Sandle, Carbon, 37: p. 1323(1999).
[14] Kukovecz A, et al., J. Phys. Chem. B, 106: p. 6374(2002).
[15] Silverstein RM, Webster FX, and Kiemle, Spectrometric Identification of Organic Compounds, 7th Edition, New York: Wiley & Sons (1988).

ER PUBLICATIONS